JOC The Journal of Organic Chemistry

pubs.acs.org/joc Article

Photochemical Release of Hydropersulfides

Sahil C. Aggarwal, Vinayak S. Khodade, Sarah Porche, Blaze M. Pharoah, and John P. Toscano*

Cite This: J. Org. Chem. 2022, 87, 12644−12652 Read Online

ACCESS | Metrics & More | Article Recommendations | Supporting Information

ABSTRACT: Hydropersulfides (RSSH) have received significant interest in the field of redox biology because of their intriguing biochemical properties. However, because RSSH are inherently unstable, their study is challenging, and as a result, the details of their physiological roles remain ill-defined. Herein, we report strategies to release RSSH utilizing photoremovable protecting groups. RSSH protection with the well-established *p*-hydroxyphenacyl (*p*HP) photoprotecting group resulted in inefficient RSSH photorelease along with complex chemistry. Therefore, an alternative precursor was examined in which a self-immolative linker was inserted between the *p*HP group and RSSH, providing nearly quantitative RSSH release following photolysis at 365 nm. Inspired by these results, we also synthesized an analogous precursor derivatized with 7-diethylaminocoumarin (DEACM), a visible light-cleavable photoprotecting group. Photolysis of this precursor at 420 nm led to efficient RSSH release, and in vitro experiments demonstrated intracellular RSSH delivery in breast cancer MCF-7 cells.

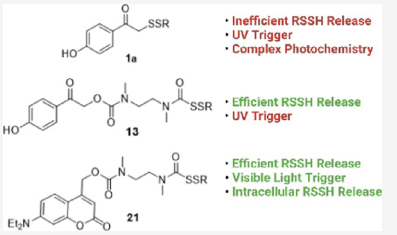

INTRODUCTION

Recent studies have revealed the prevalence and importance of hydropersulfides (RSSH) in redox biology.[1] For example, cysteine hydropersulfide (Cys-SSH) and glutathione hydropersulfide (GSSH) are abundant in mammalian cells and tissues.[2−4] The sulfurtransferase enzymes, cystathionine *β*-synthase (CBS) and cystathionine *γ*-lyase (CSE), both of which utilize cystine (Cys-SS-Cys) as a substrate, are proposed to be involved in the biosynthesis of Cys-SSH.[2,5] In addition, Cys-SSH is also produced by cysteinyl-tRNA synthetase (CARS) and subsequently translationally incorporated into proteins.[6] RSSH species possess unique chemical characteristics, including strong antioxidant,[7] reducing,[1,8] and nucleophilic properties,[9,10] that may potentially combat toxicologically relevant oxidants and electrophiles. Emerging evidence suggests that RSSH are involved in the regulation of redox signaling and antioxidant functions.[4,11−13] However, the inherently unstable nature of RSSH has limited their study.

Small molecules that can efficiently generate RSSH under physiological conditions are important research tools for investigating their roles in cellular processes.[14,15] Several donor molecules have been developed that release RSSH in the presence of specific stimuli such as cellular thiols,[16] reactive oxygen species (ROS),[17−19] pH,[20−22] and enzymes.[23−26] Interestingly, several recent studies show that pharmacological application of RSSH species can inhibit/prevent cellular damage resulting from oxidative/electrophilic stress.[7,15,27] However, many RSSH precursors suffer from limitations, including a lack of controllable release kinetics and electrophilic byproduct formation. The photochemical release of biomolecules from light-sensitive precursors has been a longstanding strategy in biological research as it offers both spatial and temporal control over the administration of effector species. For instance, Singh and co-workers have reported an *o*-nitrobenzyl protected photoprecursor to RSSH that offers spatiotemporal control over the release of *N*-acetyl *L*-cysteine hydropersulfide (NAC-SSH) (Scheme 1a).[28] However, this precursor releases potentially toxic 4,5-dimethoxy-2-nitrosobenzaldehyde and 4,5-dimethoxy-2-nitrosoacetophenone as byproducts. In addition, Singh and co-workers have also developed a visible light-triggered hydrogen disulfide (H_2S_2) photoprecursor with real-time monitoring ability of byproduct

Scheme 1. Previously Reported Light-Activated Hydropersulfide and Hydrogen Disulfide Precursors

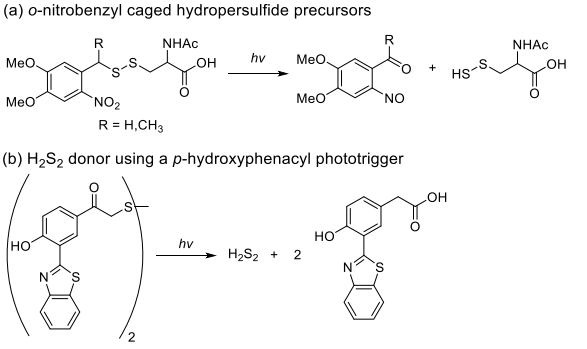

Received: May 4, 2022
Published: September 9, 2022

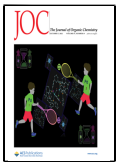

https://doi.org/10.1021/acs.joc.2c01049
J. Org. Chem. 2022, 87, 12644−12652

release with the *p*-hydroxyphenacyl benzothiazole photoprotecting group (Scheme 1b).[29]

Herein, we report our efforts to develop efficient photochemical precursors to RSSH. Owing to several advantageous properties of the *p*-hydroxyphenacyl (*p*HP) photoprotecting group, including clean photoreaction with high quantum yield and generation of *p*-hydroxyphenylacetic acid (*p*HPAA) as a benign byproduct,[30] we initially explored the use of *p*HP to mask the terminal sulfur atom of RSSH. However, inefficient RSSH release along with undesired photochemistry was unfortunately observed. Introduction of self-immolative spacer between the RSSH moiety and the *p*HP photoprotecting group improved the RSSH release efficiency. Based on these results, we also synthesized and examined an analogous precursor derivatized with 7-diethylaminocoumarin, a visible light-cleavable photoprotecting group. This photoprecursor also produces RSSH efficiently and was used to demonstrate intracellular RSSH delivery.

RESULTS AND DISCUSSION

Photoprecursor **1a**, utilizing the *p*HP photoprotecting group, was synthesized, as shown in Scheme 2. Briefly, 4-

Scheme 2. Synthesis of Hydropersulfide Precursor 1a

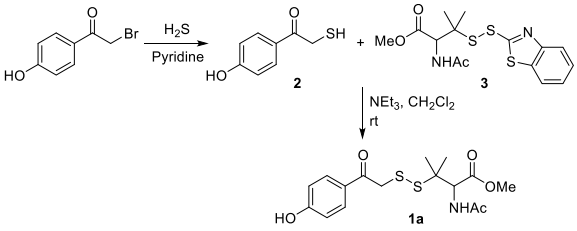

hydroxyphenacyl bromide was treated with hydrogen sulfide (H_2S) in pyridine under anhydrous conditions to obtain 4-hydroxyphenacyl thiol (**2**) in 39% yield. Thiol **2** was then treated with activated disulfide **3** in a disulfide exchange reaction to afford RSSH photoprecursor **1a**. As expected, in the absence of light, **1a** is stable in pH 7.4 phosphate-buffered saline (PBS) at ambient temperature for 24 h (Supporting Information, Figure S44).

We tested RSSH release by photolyzing (Rayonet, 350 nm) precursor **1a** (100 μM) in the presence of *S*-methyl methanethiosulfonate (MMTS, 10 equiv). MMTS was chosen because it does not have any absorbance at 350 nm and has been used previously as an efficient RSSH trap.[22,31] The photodecomposition of **1a** was monitored by ultra-performance liquid chromatography–mass spectrometry (UPLC–MS). We observe RSS-SMe (**4a**) formation, albeit in low yield, indicating some RSSH photorelease (Scheme 3). We also observe additional products including thioether **5a**, thioester **6a**, dialkyltrisulfide (S_3), and dialkyltetrasulfide (S_4), indicating that other undesired photochemical pathways are operative.

With RSSH release from **1a**, we anticipated the formation of *p*HPAA as a byproduct (Scheme 3). However, UPLC analysis shows no evidence of *p*HPAA formation. Instead, we observe the solvolysis product, *p*-hydroxyphenacyl alcohol (*p*HPOH), in 7% yield (Scheme 4, Path A). The lack of *p*HPAA formation combined with inefficient **4a** and *p*HPOH formation indicates that the desired C-S bond heterolytic cleavage pathway to release the persulfide anion is a minor contributor, analyzed by

Scheme 3. Photoproducts Observed from Precursor 1a in the Presence of MMTS

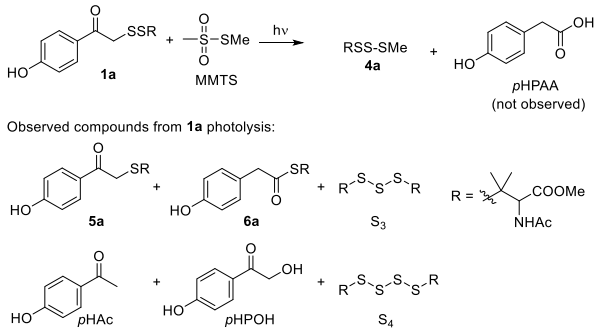

Scheme 4. Proposed Photodecomposition Pathways for 1a

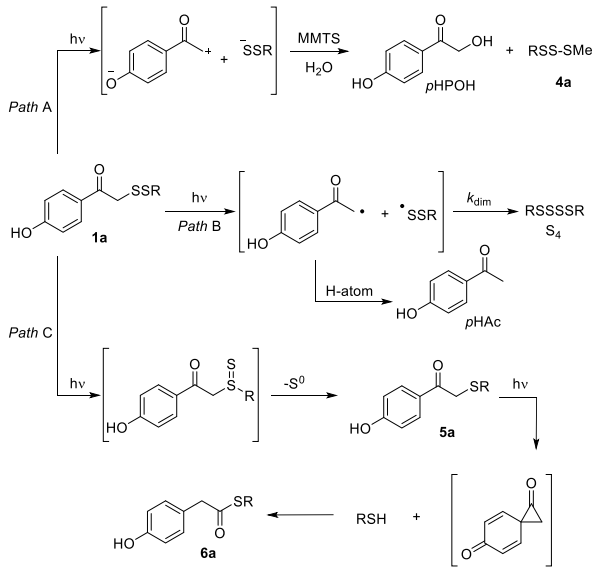

high performance liquid chromatography (HPLC) (Scheme 4, Path A). Alternatively, the C-S bond in photoprecursor **1a** may undergo homolytic cleavage to generate the *p*-hydroxyphenacyl radical and perthiyl radical (Scheme 4, Path B). Perthiyl radicals are quite unreactive and mainly dimerize to give tetrasulfides ($k = 6 \times 10^9$ M^{-1} s^{-1}).[32−34] We postulate that the formation of S_4 from **1a** photolysis is likely derived from initially produced perthiyl radicals. The *p*-hydroxyphenacyl radical can be reduced to give *p*-hydroxyacetophenone (*p*HAc).[30,35] However, HPLC analysis shows only 8% *p*HAc formation (Supporting Information, Figure S42), indicating that homolytic cleavage is also likely not a major pathway.

A time course analysis reveals that thioether **5a** is formed within 1 min of **1a** photolysis (Supporting Information, Figure S14). Furthermore, **5a** can also undergo secondary photolysis to release thiol and the presumed spirodienedione intermediate, which can subsequently react with released thiol to form thioester **6a** (Scheme 4, Path C). Hence, we measured the yield of **5a** shortly after **1a** photolysis and observed 58% formation (Supporting Information, Figure S41), indicating that thioether formation is a significant contributor.

Next, we explored the mechanism of **5a** formation. Based on previous reports, positioning of a disulfide adjacent to a carbonyl or olefin can lead to thiosulfoxide formation, which subsequently leads to sulfur extrusion and thioether generation (e.g., Scheme 4, Path C).[36−39] We tried to characterize the

https://doi.org/10.1021/acs.joc.2c01049
J. Org. Chem. 2022, 87, 12644−12652

extruded sulfur by trapping with triphenylphosphine-based probe **P2** (Figure 1).[40] However, attempts to characterize the

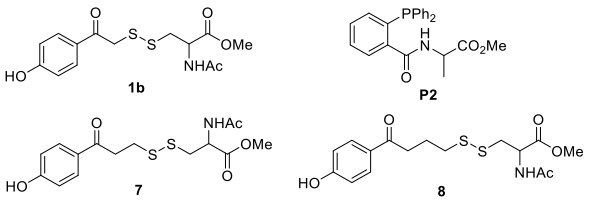

Figure 1. Cysteine analogue **1b**, triphenylphosphine-based sulfane sulfur probe **P2**, and compounds **7** and **8**.

trapped extruded sulfur were inconclusive because of the lack of selectivity of the probe toward elemental sulfur vs additional sources of sulfane sulfur (e.g., S_4, S_3, and **4a**) that are present in the reaction mixture. We also synthesized compounds **7** and **8** with a two and three methylene spacer, respectively, between the carbonyl and RSSH moiety (Figure 1) to examine potential sulfur extrusion from these compounds. Because photochemistry observed with the *p*HP photoprotecting group is highly dependent on leaving group ability, we did not expect RSSH photorelease from these compounds. Photolysis of either **7** or **8** for 1 h shows no photodecomposition along with a lack of corresponding thioether formation, analyzed by UPLC-MS (Supporting Information, Figure S25), indicating that the S-S bond in these compounds is stable to photolysis at 350 nm. Consistent with previous work,[39] these results suggest that proximity of the carbonyl relative to the disulfide is important for thioether formation. Similarly, we observe analogously complex photochemistry with cysteine analogue **1b** (Figure 1, and Supporting Information, Figure S20). Overall, these results demonstrate that direct attachment of RSSH with the *p*HP group is not a viable approach to photorelease RSSH efficiently.

Inspired by the results of lack of thioether formation from **7** and **8**, we turned to photoprecursor **13** with a self-immolative carbamate linker installed between the RSSH moiety and the *p*HP protecting group to minimize thioether formation and maximize RSSH release.[21] The synthesis of photoprecursor **13** is outlined in Scheme 5. The hydroxy group of ketone **9** was activated using 4-nitrophenyl chloroformate to obtain carbonate **10**, which was then reacted with *tert*-butyl methyl (2-(methylamino)ethyl) carbamate in the presence of triethylamine to provide compound **11** in 79% yield. Removal of the Boc protecting group using trifluoroacetic acid (TFA)

Scheme 5. Synthesis of Hydropersulfide Precursor 13

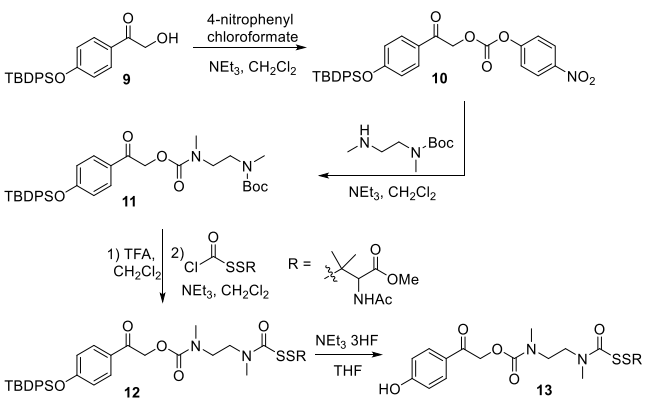

furnished the deprotected amine, which was immediately reacted with *S*-perthiocarbonyl chloride (which was obtained by *N*-acetylpenicillamine methyl ester reaction with chlorocarbonylsulfenyl chloride) in the presence of triethylamine to give **12** in 70% yield. Finally, the removal of the *tert*-butyldiphenylsilyl (TBDPS) protecting group with triethylamine trihydrofluoride afforded **13** in 84% yield. As expected, **13** is stable in pH 7.4 PBS buffer at ambient temperature in the dark over 24 h, demonstrating its stability toward hydrolysis (Supporting Information, Figure S44).

Photolysis of **13** (100 μM) at 350 nm in the presence of 10 equiv of MMTS in pH 7.4 buffer showed its disappearance over 90 min along with concomitant formation of RSS-SMe **4a**, analyzed by UPLC-MS (Figure 2). Of note, **4a** was found to be

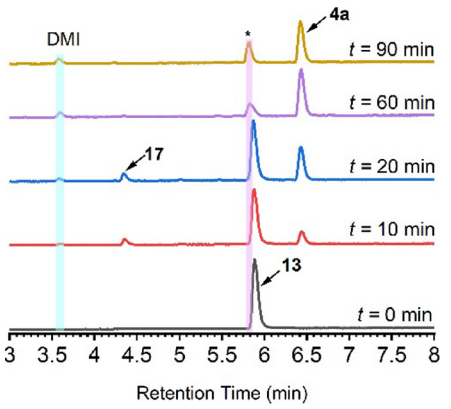

Figure 2. UPLC-MS chromatograms of RSSH trapping in ammonium bicarbonate buffer (pH 7.4, 50 mM) showing the photolysis of **13** (100 μM) at 350 nm in the presence of MMTS (1 mM) over time. Aliquots were taken at the time points indicated, quenched with 1% formic acid, and analyzed by UPLC-MS. The asterisk indicates RS-SMe formation (Supporting Information, Figure S15).

unstable under our experimental conditions (350 nm irradiation), leading to RS-SMe formation (Supporting Information, Figure S15). We also observe the expected byproduct 1,3-dimethyl-2-imidazolidinone (DMI) in 98% yield, indicating nearly quantitative release of RSSH. Moreover, HPLC analysis shows efficient formation of *p*HPAA (86%) with a small amount of *p*HPOH (6%), presumably formed via trapping of intermediate **14** with H_2O (Scheme 6) (Supporting Information, Figure S43).

Based on the observed byproducts and the extensive studies of Givens and co-workers,[35,41] we propose that **13** undergoes photocleavage to release intermediate **14** and the carbamate intermediate **15** (Scheme 6). Intermediate **14** presumably undergoes a rapid photo-Favorskii rearrangement leading to the fleeting spirodienedione intermediate **16**, which is quickly trapped by water giving *p*HPAA.[30,41] Because decarboxylation of carbamates is reported to be on the millisecond timescale under physiological conditions,[42,43] we believe that alkylamine-substituted perthiocarbamate intermediate **17** is rapidly produced. Subsequent intramolecular cyclization of **17** ($t_{1/2}$ = 1.4 min)[21] leads to efficient RSSH release and trapping by MMTS. These data also confirm that RSSH is indeed the species reacting with MMTS.

Although **13** shows efficient RSSH release, the use of UV-light as a trigger for RSSH release is not ideal because of low penetration into tissues, and long exposure may cause phototoxicity in biological systems. Hence, we synthesized

https://doi.org/10.1021/acs.joc.2c01049
J. Org. Chem. 2022, 87, 12644−12652

Scheme 6. Proposed Mechanism for Photorelease of RSSH from Precursor 13

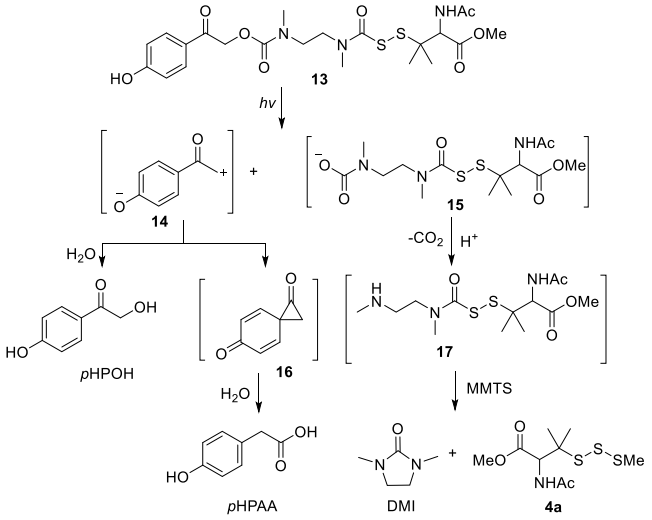

photoprecursor **21** containing the 7-diethylaminocoumarin (DEACM) photoprotecting group, which has absorption at longer wavelengths compared to the *p*HP group.[35] The synthesis of photoprecursor **21** is illustrated in Scheme 7.

Scheme 7. Synthesis of Hydropersulfide Precursor 21

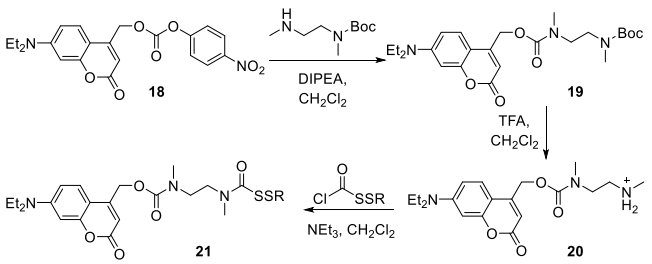

Initially, carbonate **18** was obtained using reported methods,[44] followed by reaction with *tert*-butyl methyl(2-(methylamino)-ethyl) carbamate in the presence of diisopropylethylamine (DIPEA) to produce compound **19** in 79% yield. Removal of the Boc protecting group using TFA furnished the deprotected amine **20**, which was immediately reacted with *S*-perthiocarbonyl chloride in the presence of triethylamine to provide **21** in 51% yield. As expected, **21** is found to be stable in pH 7.4 PBS buffer at ambient temperature in the dark over 48 h, demonstrating its stability toward hydrolysis (Supporting Information, Figure S45).

Photolysis of precursor **21** at 420 nm in the presence of MMTS in pH 7.4 buffer shows efficient formation of RSS-SMe **4a** (90% yield) and the expected byproduct, DMI (95% yield), analyzed by UPLC-MS. Notably, RSS-SMe was found to be stable under 420 nm irradiation. HPLC analysis shows the other expected byproduct, diethylamino coumarin alcohol (DEACM-OH), albeit in lower yield (47%). We also observe diethylamino coumarin aldehyde (DEACM-CHO) formation (10%) (Figure 3) (Supporting Information, Figure S33), likely derived from photooxidation of DEACM-OH (Scheme 8). Careful analysis of UPLC chromatograms revealed minor peaks corresponding to compounds **23** and **24**, presumably formed through trapping of cation **22** by amine **17** and persulfide anion, respectively ((Scheme 8) and Supporting

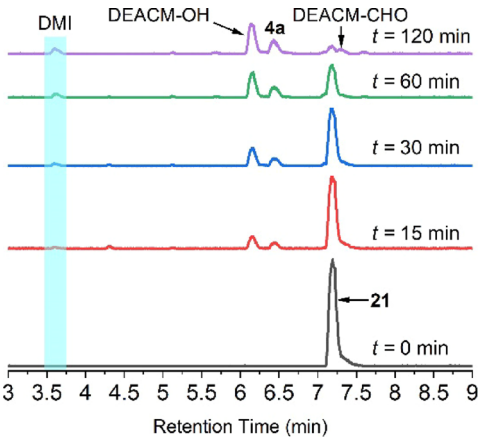

Figure 3. (a) Reaction scheme showing hydropersulfide release from **21** upon photolysis in the presence of MMTS. (b) UPLC-MS chromatograms of RSSH trapping in ammonium bicarbonate buffer (pH 7.4, 50 mM) showing the photolysis of **21** (25 μM) at 420 nm in the presence of MMTS (250 μM) over time. Aliquots were taken at the time points indicated, quenched with 1% formic acid, and analyzed by UPLC-MS.

Information, Figure S33). An additional minor peak corresponding to thioether **25** is also observed, likely derived from secondary photolysis of disulfide **24** via sulfur extrusion. These additional products account for the low yield of DEACM-OH. The quantum yield of disappearance of **21** was found to be $\Phi = 0.27 \pm 0.06$ using the potassium ferrioxalate actinometer.[45,46]

To determine the potential utility of **21** for biological applications, we first examined its reactivity with thiols. About 86% of **21** remains following incubation with 5 equiv of *N*-acetylcysteine in PBS (pH 7.4) for 2 h at 37 °C (Supporting Information, Figure S46), indicating the suitability of this precursor for biological studies.

We then sought to determine whether **21** can release RSSH in cells following photolysis as a trigger. The cytotoxicity of **21** on MCF-7 cells using the Cell Counting Kit-8 (CCK-8) assay reveals no toxicity at concentrations up to 50 μM (Supporting Information, Figure S47). Also, the DMI and DEACM-OH byproducts at 50 μM exhibited no cytotoxicity (Supporting Information, Figure S47). In addition, photolysis at 420 nm (1500 W, LED lamp) for 45 min has no effect on MCF-7 cell viability (Supporting Information, Figure S48). Next, we measured the ability of **21** to photorelease RSSH within cells using SSP4 (Figure 4b), an established fluorescent probe that has been used to detect intracellular sulfane sulfur levels qualitatively.[47] When MCF-7 cells are pretreated with **21** for 20 min and photolyzed with 420 nm light, we observe a clear increase in SSP4-derived fluorescence (Figure 4a), indicating intracellular RSSH release. Released RSSH in cells may also undergo a disproportionation reaction leading to polysulfide formation, which can also react with SSP4 to give a fluorescence signal. Next, we compared RSSH release efficiency of **21** with RSSH precursor **26** (Figure 4b) under similar experimental conditions. Precursor **26** undergoes neutralization under physiological conditions to produce intermediate **17** (the same intermediate also produced following photolysis of precursor **21**) that releases RSSH. Importantly, the SSP4 fluorescence signal in the case of photoprecursor **21** is much higher compared to its non-photoprotected analogue **26**.[21] The short half-life of precursor **26** (1.4 min) can lead to relatively rapid decomposition prior

https://doi.org/10.1021/acs.joc.2c01049
J. Org. Chem. 2022, 87, 12644−12652

Scheme 8. Proposed Mechanism of RSSH Release from Precursor 21

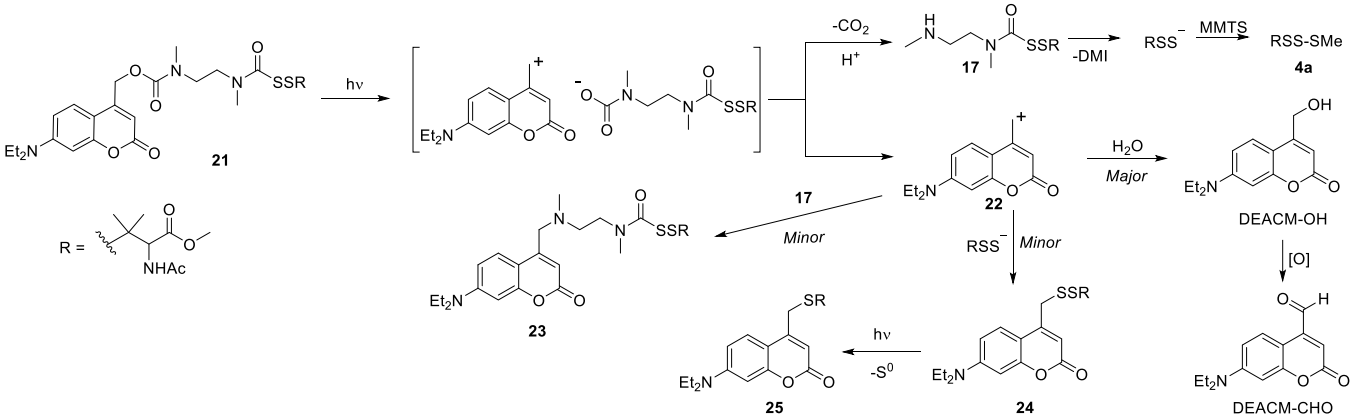

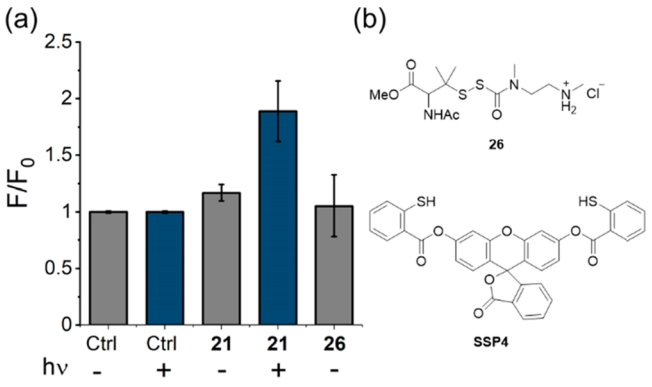

Figure 4. (a) Intracellular RSSH release in MCF-7 epithelial cells. MCF-7 cells were pretreated with RSSH photoprecursor **21** and precursor **26** at 25 μM and incubated for 20 min at 37 °C. Cells were exposed to 420 nm light for 30 min and then treated with SSP4 (10 μM) and CTAB (100 μM) for 20 min at 37 °C. Fluorescence intensity was measured at Ex 482 nm Em 515, and results are expressed as the mean ± SEM (n = 3 for each treatment group) with three independent experiments. (b) Structure of RSSH precursor **26** and sulfane sulfur probe SSP4.

to intracellular uptake, which results in a lower SSP4 response. Thus, DECAM photoprecursor **21** provides utility by enhancing intracellular RSSH delivery over its nonphotoprotected analog.

CONCLUSIONS

Herein, we describe photoprecursor optimization to enable efficient RSSH release in a controlled manner. Complex photochemistry is observed with direct attachment of RSSH to the *p*HP protecting group. Therefore, we incorporated a self-immolative linker, which leads to clean and efficient RSSH release along with the formation of the expected byproducts, pHPAA and DMI. We also synthesized visible light-activated precursor **21** that releases RSSH following photolysis at 420 nm. Moreover, we demonstrate that photoprecursor **21** can release RSSH in MCF-7 cells as measured by the SSP4 fluorescence probe. We also tested compound **26**, which lacks the photoprotecting group, but analogously releases RSSH, and find that it is unable to increase intracellular RSSH levels. We hope that visible light photoprecursor **21** will find use as a research tool for the spatiotemporal delivery of RSSH to aid our understanding of RSSH chemical biology.

EXPERIMENTAL PROCEDURES

General Information. Analytical thin layer chromatography (TLC) was performed on silica gel on TLC Al foils with fluorescent indicator F254 plates (Sigma-Aldrich). Visualization was accomplished with UV light (254 nm) or staining with $KMnO_4$. Starting materials, solvents, and reagents were received from commercial sources (Sigma-Aldrich, Oakwood Chemical, and TCI), unless otherwise noted and were used without purification. Deuterated solvents (Cambridge Isotope Laboratories) were used for NMR spectroscopic analyses. NMR spectra were obtained on a Bruker 400 MHz NMR spectrometer. In the case of ^{1}H NMR in $CDCl_3$, chemical shifts are reported relative to tetramethylsilane (δ = 0). The other spectra are referenced internally according to residual solvent signals of deuterated chloroform ($CDCl_3$, ^{13}C NMR; δ = 77.16 ppm), DMSO-d_6 (^{1}H NMR; δ = 2.50 ppm, ^{13}C NMR; δ = 39.52 ppm), and deuterated acetonitrile (ACN-d_3, ^{1}H NMR; δ = 1.94 ppm, ^{13}C NMR; δ = 1.32 ppm, 118 ppm). Photolyses were carried out either with a Rayonet Photochemical Mini-Reactor Model RMR-600 utilizing 6 × RMR-3500A° lamps or Designers Edge model L-1923 1500 W, LED lamp. Photolyses were carried out in borosilicate glass vials for compound **21** and quartz cuvettes for compounds **1a** and **13**. High-resolution mass spectra were obtained on a Waters Acquity Q-ToF MS/MS instrument. The products of RSSH release from compounds **1a**, and **13** were quantified using a high-performance liquid chromatography (HPLC, Agilent 1100 series) system with a Phenomenex C-18 reverse phase column (250 mm × 4.6 mm, 5 μm). UPLC−MS analysis was carried out with a Waters Acquity/Xevo-G2 UPLC-MS system equipped with an ACQUITY UPLC BEH C18 column (2.1 mm × 50 mm, 1.7 μm). The mass signals for products of RSSH trapping with *S*-methylmethanethiosulfonate (MMTS) were obtained via deconvolution using MassLynx 4.1 software. In addition to the protonated molecule $[M + H]^+$, we also observe $[M + Na]^+$ adducts during ESI-MS analysis. MCF-7 human epithelial cells were obtained from the American Type Culture Collection. Cells were grown in Dulbecco's minimal essential medium (DMEM), supplemented with fetal bovine serum (FBS) 10%, penicillin 100 U/mL, and streptomycin 100 μg/mL. The pH measurements were performed using a Fisher Scientific Accumet AB15 pH meter. The photolysis of cells was carried out with a Designers Edge model L-1923 (1500 W) LED lamp. Fluorescence readings of cells in 96 well plates were measured on SpectraMax M2 and SpectraMax M2e Multidetection Readers.

Experimental Procedure and Spectroscopic Data. *1-(4-Hydroxyphenyl)-2-mercaptoethan-1-one (2).* This compound was prepared according to the literature report.[48] A 1 M solution of 4-hydroxyphenacyl bromide (3.5 g, 16.36 mmol, 1 equiv) in tetrahydrofuran (THF) was transferred dropwise at −15 °C to a solution of pyridine (35 mL) purged with H_2S gas. The resulting mixture was stirred for an additional 10 min with continuous purging of H_2S gas. Upon completion of the reaction (analyzed by TLC), the solution was brought to 0 °C and quenched with cold 1 M HCl. The

https://doi.org/10.1021/acs.joc.2c01049
J. Org. Chem. 2022, 87, 12644−12652

aqueous layer was extracted with ethyl acetate (3 × 60 mL). The combined organics were washed with brine and dried over Na_2SO_4. The volatiles were removed under reduced pressure, and the crude material was purified with flash column chromatography on silica gel with 50% ethyl acetate in hexanes as the eluent to give **2** as a white solid (1.06 g, 39% yield). ^{1}H NMR (400 MHz, DMSO) δ 10.42 (s, 1H), 7.86 (d, J = 8.7 Hz, 2H), 6.85 (d, J = 8.8 Hz, 2H), 3.97 (d, J = 6.9 Hz, 2H), 2.77 (t, J = 7.2 Hz, 1H). ^{13}C {1H} NMR (101 MHz, DMSO) δ 194.2, 162.8, 131.6, 126.9, 115.8, 30.6.

*Methyl 2-Acetamido-3-((2-(4-hydroxyphenyl)-2-oxoethyl)-disulfaneyl)-3-methylbutanoate (**1a**).* Methyl 2-acetamido-3-(benzo[*d*]thiazol-2-yldisulfaneyl)-3-methylbutanoate (220 mg, 0.59 mmol, 1 equiv) was added in one portion to a solution of **2** (100 mg, 0.59 mmol, 1 equiv) in dichloromethane (6 mL). Triethylamine (90 mg, 124 μL, 0.89 mmol, 1.5 equiv) was added dropwise over 1 min and stirred for an additional 30 min at room temperature. Upon completion of the reaction (analyzed by TLC), the reaction was quenched with 1 M HCl, and the aqueous layer was extracted with ethyl acetate (3 × 10 mL). The combined organics were washed with brine and dried over Na_2SO_4. The volatiles were removed under reduced pressure, and the crude was purified via flash column chromatography on silica gel with 60% ethyl acetate in hexanes as the eluent to give **1a** as a white solid (50 mg, 23% yield). ^{1}H NMR (400 MHz, DMSO) δ 10.43 (s, 1H), 8.26 (d, J = 8.7 Hz, 1H), 7.82 (d, J = 8.9 Hz, 2H), 6.84 (d, J = 8.9 Hz, 2H), 4.58 (d, J = 8.8 Hz, 1H), 4.30−4.11 (m, 2H), 3.61 (s, 3H), 1.87 (s, 3H), 1.32 (s, 3H), 1.29 (s, 3H). ^{13}C {1H} NMR (101 MHz, CD_3CN) δ 193.6, 171.4, 171.1, 162.8, 132.1, 128.7, 116.2, 59.4, 52.9, 52.6, 47.2, 25.8, 24.3, 22.7. HRMS (ESI): m/z calcd for $C_{16}H_{22}NO_5S_2^+$ [M + H]$^+$ 372.0934, found 372.0943.

*Methyl 2-Acetamido-3-((2-(4-hydroxyphenyl)-2-oxoethyl)thio)-3-methylbutanoate (**5a**).* Methyl 2-acetamido-3-mercapto-3-methylbutanoate (157 mg, .77 mmol, 1.1 equiv) was added to a solution of 2-bromo-1-(4-hydroxyphenyl)ethan-1-one (150 mg, 0.70 mmol, 1 equiv) in THF (7 mL). Triethylamine (106 mg, 146 μL, 1.05 mmol, 1.5 equiv) was added dropwise over 1 min, and the reaction was stirred at room temperature for 1 h. The volatiles were removed under reduced pressure. The crude was redissolved in ethyl acetate (20 mL), washed with brine, and dried over Na_2SO_4. The volatiles were removed under reduced pressure, and the crude was purified via flash column chromatography on silica gel with 60% ethyl acetate in hexanes as the eluent to give compound **5a** as a white solid (100 mg, 42% yield). ^{1}H NMR (400 MHz, $CDCl_3$) δ 7.88 (d, J = 8.8 Hz, 2H), 7.47 (s, 1H), 6.89 (d, J = 8.8 Hz, 2H), 6.81 (d, J = 8.8 Hz, 1H), 4.69 (d, J = 8.7 Hz, 1H), 4.07−3.92 (m, 2H), 3.74 (s, 3H), 2.13 (s, 3H), 1.46 (s, 3H), 1.45 (s, 3H). ^{13}C {1H} NMR (101 MHz, DMSO) δ 194.3, 171.0, 170.1, 162.8, 131.6, 127.5, 115.7, 58.9, 52.2, 47.5, 35.7, 26.1, 25.5, 22.7. HRMS (ESI): m/z calcd for $C_{16}H_{22}NO_5S$+ [M + H] + 340.1213, found 340.1211.

*Methyl N-Acetyl-S-((2-(4-hydroxyphenyl)-2-oxoethyl)thio)-cysteinate (**1b**).* This compound was synthesized similar to **1a**. Briefly, triethylamine (176 mg, 242 μL, 1.74 mmol, 1.5 equiv) was added dropwise over 2 min to a solution of 3 (195 mg, 1.16 mmol, 1 equiv) and methyl *N*-acetyl-S-(pyridin-2-ylthio)cysteinate (333 mg, 1.16 mmol, 1 equiv) in DCM (12 mL) and stirred at room temperature for 1 h. Upon completion of the reaction (analyzed by TLC), the reaction was quenched with DI water and the aqueous layer was extracted with DCM (3 × 10 mL). The combined organics were washed with brine and dried over Na_2SO_4. The volatiles were removed under reduced pressure, and the crude was purified via flash column chromatography on silica gel with 70% ethyl acetate in hexanes as the eluent to give compound **1b** as a white solid (200 mg, 50% yield). ^{1}H NMR (400 MHz, DMSO) δ 10.46 (s, 1H), 8.40 (d, J = 7.4 Hz, 1H), 7.86 (d, J = 8.8 Hz, 2H), 6.85 (d, J = 8.8 Hz, 2H), 4.57−4.48 (m, 1H), 4.36−4.21 (m, 2H), 3.61 (s, 3H), 3.13−3.06 (m, 1H), 2.99−2.80 (m, 1H), 1.84 (s, 3H). ^{13}C {1H} NMR (101 MHz, DMSO) δ 193.3, 171.5, 170.0, 162.9, 131.8, 127.2, 115.8, 105.0, 52.6, 51.5, 44.9, 22.8. HRMS (ESI): m/z calcd for $C_{14}H_{18}NO_5S_2^+$ [M + H]$^+$ 344.0621, found 344.0627.

*Methyl N-Acetyl-S-((3-(4-hydroxyphenyl)-3-oxopropyl)thio)-cysteinate (**7**).* *N*-Acetylcysteine methyl ester (73 mg, 0.41 mmol) was added to a solution of **23** (100 mg, 0.34 mmol, 1 equiv) in DCM (5 mL) at room temperature and stirred for 5 min. Triethylamine (52 mg, 72 μL, 0.52 mmol, 1.5 equiv) was added dropwise over 1 min and stirred at room temperature for 30 min. Upon completion of the reaction (analyzed by TLC), the reaction was quenched with DI water and the aqueous layer was extracted with ethyl acetate (3 × 20 mL). The combined organics were washed with brine and dried over Na_2SO_4. The volatiles were removed under reduced pressure, and the crude was purified via flash column chromatography on silica gel with 50% ethyl acetate in hexanes as the eluent to give **7** as a semisolid (40 mg, 33% yield). ^{1}H NMR (400 MHz, $CDCl_3$) δ 7.92 (d, J = 8.8 Hz, 2H), 6.92 (d, J = 8.8 Hz, 2H), 6.53 (d, J = 7.6 Hz, 1H), 4.95−4.91 (m 1H), 3.80 (s, 3H), 3.37−3.33 (m, 2H), 3.28−3.18 (m, 2H), 3.11 (t, J = 6.9 Hz, 2H), 2.11 (s, 3H). ^{13}C {1H} NMR (101 MHz, $CDCl_3$) δ 196.9, 171.2, 170.9, 161.9, 130.7, 128.8, 115.7, 52.9, 52.1, 40.1, 37.6, 32.9, 23.0. HRMS (ESI): m/z calcd for $C_{15}H_{20}NO_5S_2^+$ [M + H]$^+$ 358.0777, found 358.0772.

*Methyl N-Acetyl-S-((4-(4-hydroxyphenyl)-4-oxobutyl)thio)-cysteinate (**8**).* This compound was prepared according to the procedure used for compound **7**. *N*-Acetyl cysteine methyl ester (94 mg, 0.53 mmol, 1.2 equiv), **25** (135 mg, 0.44 mmol, 1 equiv), and NEt_3 (67 mg, 92 μL, 0.66 mmol, 1.5 equiv) were added in DCM (5 mL). Upon completion of the reaction (analyzed by TLC), the reaction was quenched with DI water and the aqueous layer was extracted with ethyl acetate (3 × 20 mL). The combined organics were washed with brine and dried over Na_2SO_4. The volatiles were removed under reduced pressure, and the crude was purified via flash column chromatography on silica gel with 50% ethyl acetate in the hexane eluent to give **8** as a semisolid (70 mg, 42% yield). ^{1}H NMR (400 MHz, DMSO) δ 10.34 (s, 1H), 8.45 (d, J = 7.9 Hz, 1H), 7.85 (d, J = 8.8 Hz, 2H), 6.85 (d, J = 8.8 Hz, 2H), 4.63−4.50 (m, 1H), 3.63 (s, 3H), 3.13−3.05 (m, 1H), 3.03 (t, J = 7.1 Hz, 2H), 2.97−2.88 (m, 1H), 2.78 (t, J = 7.2 Hz, 2H), 1.99−1.90 (m, 2H), 1.86 (s, 3H). ^{13}C {1H} NMR (101 MHz, $CDCl_3$) δ 198.6, 171.3, 171.0, 161.8, 130.7, 129.0, 115.6, 52.9, 52.0, 40.2, 38.0, 36.1, 23.4, 23.0. HRMS (ESI): m/z calcd for $C_{16}H_{22}NO_5S_2^+$ [M + H]$^+$ 372.0934, found 372.0927.

*2-(4-((tert-Butyldiphenylsilyl)oxy)phenyl)-2-oxoethyl (4-Nitrophenyl) Carbonate (**10**).* 1-(4-((*tert*-Butyldiphenylsilyl)oxy)phenyl)-2-hydroxyethan-1-one (**9**) was synthesized according to the literature procedure without any alterations.[49] A 1 M solution of 4-nitrophenyl chloroformate (774 mg, 3.84 mmol, 1.5 equiv) was transferred dropwise over 5 min to a solution **9** (1.0 g, 2.56 mmol, 1 equiv) in DCM (10 mL) at 0 °C and stirred for another 5 min. Triethylamine (415 mg, 571 μL, 4.10 mmol, 1.6 equiv) was added dropwise over 5 min at 0 °C, and the reaction was stirred overnight. Upon completion of the reaction (analyzed by TLC), the reaction was quenched with DI water and the aqueous layer was extracted with DCM (3 × 10 mL). The combined organics were washed with brine and dried over Na_2SO_4. The volatiles were removed under reduced pressure, and the crude was purified via flash column chromatography on silica gel with 10% ethyl acetate in hexanes as the eluent to give **10** as a white flaky solid (400 mg, 28% yield). ^{1}H NMR (400 MHz, $CDCl_3$) δ 8.30 (d, J = 9.3 Hz, 2H), 7.80−7.68 (m, 6H), 7.53−7.36 (m, 8H), 6.87 (d, J = 8.8 Hz, 2H), 5.40 (s, 2H), 1.14 (s, 9H). ^{13}C {1H} NMR (101 MHz, $CDCl_3$) δ 189.2, 161.1, 155.6, 152.4, 135.4, 131.8, 130.3, 129.8, 128.0, 126.9, 125.3, 121.8, 120.2, 105.0, 69.2, 26.4, 19.5. HRMS (FAB): m/z calcd for $C_{31}H_{29}NO_7Si$ [M + H]$^+$ 556.1786, found 556.1799.

*tert-Butyl (2-(4-((tert-Butyldiphenylsilyl)oxy)phenyl)-2-oxoethyl) Ethane-1,2-diylbis(methylcarbamate) (**11**).* *tert*-Butyl methyl(2-(methylamino)ethyl)carbamate (457 mg, 2.58 mmol) was added to a solution of 10 (718 mg, 1.29 mmol, 1 equiv) in DCM (13 mL) at 0 °C and stirred for 10 min at the same temperature. Diisopropylethylamine (501 mg, 675 μL, 3.88 mmol, 3 equiv) was added dropwise and stirred at room temperature for 2 h. Upon completion of the reaction (analyzed by TLC), the reaction was quenched with DI water and the aqueous layer was extracted with DCM (3 × 20 mL). The combined organics were washed with brine and dried over Na_2SO_4. The volatiles

https://doi.org/10.1021/acs.joc.2c01049
J. Org. Chem. 2022, 87, 12644−12652

were removed under reduced pressure and the crude was purified via flash column chromatography on silica gel with 40% ethyl acetate in hexanes as eluent to give **11** (mixture of rotamers) as a clear viscous oil (618 mg, 79%). ^{1}H NMR (400 MHz, $CDCl_3$) δ 7.77−7.67 (m, 6H), 7.49−7.36 (m, 6H), 6.83 (d, J = 8.7 Hz, 2H), 5.31−5.20 (m, 2H), 3.56−3.34 (m, 4H), 3.06 (s, 1H), 2.99 (s, 2H), 2.92 (s, 3H), 1.47 (s, 9H), 1.13 (s, 9H). ^{13}C {1H} NMR (101 MHz, $CDCl_3$) δ 191.8, 160.6, 155.6, 135.4, 132.0, 130.2, 129.7, 128.0, 127.7, 120.0, 66.5, 47.2, 35.7, 28.4, 26.4, 19.5. HRMS (ESI): m/z calcd for $C_{34}H_{44}N_2O_6Si^+$ $[M + H]^+$ 605.3041, found 605.3046.

*Methyl 13-Acetamido-1-(4-((tert-butyldiphenylsilyl)oxy)phenyl)-5,8,12,12-tetramethyl-1,4,9-trioxo-3-oxa-10,11-dithia-5,8-diazatetradecan-14-oate (**12**).* Trifluoroacetic acid (3 mL) was added dropwise over 1 min to a solution of **11** (410 mg, 0.68 mmol, 1 equiv) in DCM (3 mL) at 25 °C. The reaction was stirred at room temperature for 45 min. Upon completion of the reaction (analyzed by TLC) the volatiles were removed under reduced pressure and used immediately for the next step.

***S*-Perthiocarbonyl Chloride.** A 1 M solution of chlorocarbonylsulfenyl chloride (75 mg, 48 μL, 0.57 mmol, 1.3 equiv) was added dropwise over 2 min to a solution of methyl 2-acetamido-3-mercapto-3-methylbutanoate (90 mg, 0.44 mmol, 1 equiv) in DCM (5 mL) at 0 °C, the reaction was stirred at 0 °C for 45 min. The volatiles were removed under reduced pressure at room temperature and used immediately for the next step.

A 1 M solution of *S*-perthiocarbonyl chloride (146 mg, 0.49 mmol) in DCM was transferred to a cold solution of 2-(((2-(4-((*tert*-butyldiphenylsilyl)oxy)phenyl)-2-oxoethoxy)carbonyl)(methyl)-amino)-*N*-methylethan-1-aminium 2,2,2 trifluoroacetate (391 mg, 0.63 mmol, 1 equiv) in DCM (5 mL) and stirred for 5 min. Triethylamine (74 mg, 102 μL, 0.73 mmol, 1.2 equiv) was added dropwise at 0 °C and stirred for 30 min at room temperature. Upon completion of the reaction (analyzed by TLC), the reaction was quenched with DI water and the aqueous layer was extracted with DCM (3 × 20 mL). The combined organics were washed with brine and dried over Na_2SO_4. The volatiles were removed under reduced pressure and the crude was purified via flash column chromatography on silica gel with 70% ethyl acetate in hexanes as eluent to give **12** (mixture of rotamers) as a clear viscous oil (260 mg, 70% yield over 2 steps). ^{1}H NMR (400 MHz, $CDCl_3$) δ 7.78−7.66 (m, 6H), 7.56 (s, 1H), 7.51−7.35 (m, 6H), 6.82 (d, J = 8.7 Hz, 2H), 5.38−5.11 (m, 2H), 4.56 (d, J = 8.3 Hz, 1H), 3.79−3.69 (m, 4H), 3.68−3.43 (m, 3H), 3.24−2.95 (m, 6H), 2.06 (s, 3H), 1.47 (s, 3H), 1.35 (s, 3H), 1.12 (s, 9H). ^{13}C {1H} NMR (101 MHz, $CDCl_3$) δ 191.7, 170.4, 160.7, 135.4, 135.4, 132.0, 130.3, 129.7, 128.0, 127.6, 120.0, 66.6, 60.4, 59.3, 52.5, 52.1, 48.3, 26.5, 26.4, 26.0, 22.9, 19.4. HRMS (ESI): m/z calcd for $C_{38}H_{49}N_3O_8S_2Si^+$ $[M + H]^+$ 768.2803, found 768.2807.

*Methyl 13-Acetamido-1-(4-hydroxyphenyl)-5,8,12,12-tetramethyl-1,4,9-trioxo-3-oxa-10,11-dithia-5,8-diazatetradecan-14-oate (**13**).* Triethylamine trihydrofluoride (76 mg, 77 μL, 0.47 mmol, 1.5 equiv) was added dropwise to a solution of **12** (241 mg, 0.31 mmol, 1 equiv) in THF (3 mL) at 0 °C and stirred at room temperature for 1 h. Upon completion of the reaction (analyzed by TLC), the volatiles were removed under reduced pressure. The crude was redissolved in ethyl acetate (10 mL) and washed with brine and dried over Na_2SO_4. The volatiles were removed under reduced pressure and the crude was purified via flash column chromatography on silica gel with 90% ethyl acetate in hexanes as the eluent to give compound **13** (mixture of rotamers) as a white solid (140 mg, 84% yield). ^{1}H NMR (400 MHz, CD_3CN) δ 8.20 (s, 1H), 7.86 (d, J = 8.7 Hz, 2H), 7.50 (d, J = 7.2 Hz, 1H), 6.92 (d, J = 8.7 Hz, 2H), 5.40−5.10 (m, 2H), 4.61−4.39 (m, 1H), 3.76−3.62 (m, 4H), 3.65−3.42 (m, 3H), 3.22−2.82 (m, 5H), 1.97 (s, 3H), 1.38 (s, 3H), 1.32 (s, 3H). ^{13}C {1H} NMR (101 MHz, CD_3CN) δ 192.1, 170.4, 170.3, 162.0, 155.4, 130.2, 126.7, 115.4, 66.8, 59.2, 52.0, 51.7, 25.1, 24.4, 21.8. HRMS (ESI): m/z calcd for $C_{22}H_{32}N_3O_8S_2^+$ $[M + H]^+$ 530.1625, found 530.1636.

*tert-Butyl ((7-(Diethylamino)-2-oxo-2H-chromen-4-yl)methyl) Ethane-1,2-diylbis(methylcarbamate) (**19**).* A solution of *tert*-butyl methyl(2-(methylamino)ethyl)carbamate (342 mg, 1.82 mmol, 1.5 equiv) in DCM (7 mL) was added to a solution of (7-(diethylamino)-2-oxo-2H-chromen-4-yl)methyl (4-nitrophenyl) carbonate (**18**) (500 mg, 1.21 mmol, 1 equiv) in DCM (20 mL) at 0 °C and stirred for 5 min at the same temperature. Diisopropylethylamine (235 mg, 307 μL, 1.82 mmol, 1.5 equiv) was added dropwise and stirred at room temperature for 2.5 h. Upon completion of the reaction (analyzed by TLC), the reaction was quenched with DI water and the aqueous layer was extracted with DCM (3 × 10 mL). The combined organics were washed with brine and dried over Na_2SO_4. The volatiles were removed under reduced pressure and the crude was purified via flash column chromatography on silica gel with 50% ethyl acetate in hexanes as the eluent to give **19** (mixture of rotamers) as a yellow semisolid (618 mg, 79%); ^{1}H NMR (300 MHz, $CDCl_3$) δ 7.29 (d, J = 9.0 Hz, 1H), 6.56 (dd, J = 9.0, 2.5 Hz, 1H), 6.49 (d, J = 2.5 Hz, 1H), 6.10 (s, 1H), 5.24 (d, J = 3.8 Hz, 2H), 3.57−3.30 (m, 8H), 3.00 (s, 3H), 2.87 (s, 3H), 1.43 (s, 9H), 1.19 (t, J = 7.1 Hz, 6H); ^{13}C {1H} NMR (101 MHz, $CDCl_3$) δ 162.0, 161.9, 156.3, 156.2, 155.5, 150.7, 150.4, 124.5, 124.4, 108.7, 106.0, 97.8, 79.7, 62.5, 62.4, 46.9, 46.6, 46.0, 44.7, 36.0, 34.9, 34.6, 28.4, 12.4; HRMS (ESI): m/z calcd for $C_{24}H_{35}N_3O_6^+$ $[M + H]^+$ 462.2599, found 462.2595.

*Methyl 12-Acetamido-1-(7-(diethylamino)-2-oxo-2H-chromen-4-yl)-4,7,11,11-tetramethyl-3,8-dioxo-2-oxa-9,10-dithia-4,7-diazatridecan-13-oate (**21**).* Trifluoroacetic acid (1 mL) was added dropwise over 1 min to a solution of **19** (407 mg, 0.88 mmol, 1 equiv) in DCM (10 mL) at 25 °C. The reaction was stirred at room temperature for 45 min. Upon completion of the reaction (analyzed by TLC), the volatiles were removed under reduced pressure to obtain 2-((((7-(diethylamino)-2-oxo-2H-chromen-4-yl)methoxy)-carbonyl)(methyl)amino)-*N*-methylethan-1-aminium 2,2,2-trifluoroacetate (**20**), which was used immediately for the next step. A 1 M solution of methyl 2-acetamido-3-((chlorocarbonyl)disulfaneyl)-3-methylbutanoate (264 mg, 0.88 mmol, 1 equiv) in DCM was transferred to a cold solution of **20** (419 mg, 0.88 mmol, 1 equiv) in DCM (5 mL) and stirred for 5 min. Triethylamine (196 mg, 269 μL, 1.94 mmol, 2.2 equiv) was added dropwise at 0 °C and stirred for 60 min at room temperature. Upon completion of the reaction (analyzed by TLC), the reaction was quenched with DI water and the aqueous layer was extracted with DCM (3 × 20 mL). The combined organics were washed with brine and dried over Na_2SO_4. The volatiles were removed under reduced pressure, and the crude was purified via flash column chromatography on silica gel with 80% ethyl acetate in hexanes as the eluent to give **21** (mixture of rotamers) as a yellow solid (283 mg, 51% yield over 2 steps). ^{1}H NMR (400 MHz, $CDCl_3$) δ 7.42 (bs, 1H), 7.31 (d, J = 8.9 Hz, 1H), 6.58 (dd, J = 9.0, 2.5 Hz, 1H), 6.51 (d, J = 2.5 Hz, 1H), 6.09 (s, 1H), 5.24 (d, J = 5.3 Hz, 2H), 4.53 (d, J = 8.4 Hz, 1H), 3.72 (s, 3H), 3.66−3.49 (m, 4H), 3.41 (q, J = 7.1 Hz, 4H), 3.14−3.01 (m, 6H), 2.07 (s, 3H), 1.45 (s, 3H), 1.33 (s, 3H), 1.20 (t, J = 7.1 Hz, 6H); ^{13}C {1H} NMR (101 MHz, $CDCl_3$) δ 170.4, 167.4, 162.0, 161.9, 156.3, 156.2, 155.6, 150.7, 150.7, 150.3, 124.5, 124.4, 108.7, 106.0, 105.9, 97.7, 62.5, 59.2, 53.5, 52.5, 52.1, 48.1, 46.5, 44.7, 36.0, 35.6, 34.7, 26.4, 25.7, 22.9, 12.4;. HRMS (ESI): m/z calcd for $C_{28}H_{40}N_4O_8S_2^+$ $[M + H]^+$ 625.2360, found 625.2369.

General Procedure of Photolysis of RSSH Precursors. In general, RSSH precursors and MMTS were dissolved in DMSO to afford a 10 mM and 50 mM stock, respectively, unless stated otherwise. Briefly, MMTS (10 equiv) and precursor (1 equiv) were added in pH 7.4 ammonium bicarbonate (50 mM, 4.85 mL) buffer. The mixture was pre-incubated for 10 min at 37 °C. An aliquot of the resulting solution (3 mL) was transferred to a quartz cuvette and photolyzed with 6 × RMR-3500A° lamps in a Rayonet Photochemical Mini-Reactor Model RMR-600 or with a Designers Edge model L-1923 (1500 W) LED lamp for the desired time. The protocol for LED irritation followed a literature procedure.[50] Samples were irradiated from a distance of 10−15 cm. An aliquot of the reaction mixture (500 μL) was withdrawn at specified time points and transferred to precooled 1% formic acid (500 μL) and analyzed using UPLC-MS or HPLC (see the Supporting Information for more details).

Cell Culture. MCF-7 human epithelial cells were obtained from the American Type Culture Collection. Cells were grown in Dulbecco's minimal essential medium (DMEM), supplemented with fetal bovine serum (FBS) 10%, penicillin 100 U/mL, and

https://doi.org/10.1021/acs.joc.2c01049
J. Org. Chem. 2022, 87, 12644−12652

streptomycin 100 μg/mL. They were propagated in T75-flasks, split before reaching 70−80% confluence (usually every day or every second day). Cells were passaged to black/clear bottom tissue culture-treated 96-well microtiter plates at the specified density in 180 μL volumes and incubated for 24 h.

Cytotoxicity Study of 21. Cells were seeded at a density of 2.5 × 10^4 cells/well. After 24 h, the media was replaced and compound **13** was added in 20 μL volumes using DMSO:H_2O (<0.01% DMSO) as the vehicle. Cells were incubated for an additional 24 h before media was removed and washed twice with PBS (pH 7.4). Then, 100 μL of media containing 10% v/v CCK-8 (DoJindo) was added and the cells were incubated for 3 h prior to obtaining absorbance at 450 nm. The relative % viability was calculated as 100 times the ratio of the Abs450 (cells treated with compound 10−100 μM) over Abs450 (vehicle treated).

Hydropersulfide Delivery and Intracellular Detection with SSP4. Cells were seeded at a density of 2.5 × 10^4 cells/well. After 24 h, the media is removed, then, 25 μM **21** and **26** (prepared by previous methods) are introduced to the cells and incubated for 20 min at 37 °C and 5% CO_2. Media was aspirated gently and washed with DMEM, high glucose, and HEPES (phenol red and serum free) twice. The cells were then photolyzed in the same media with a Designers Edge model L-1923 (1500 W) for 30 min. The cells were then subsequently washed twice with serum free media and treated with 10 μM SSP4 and 100 μM CTAB in a 100 μL volume and incubated at 37 °C for 20 min. The SSP4/CTAB solution was removed, and the cells were washed two times with fresh HBSS. Finally, 100 μL of HBSS is added to the wells, and the fluorescence readings were obtained at 482 Ex/515 Em.

■ ASSOCIATED CONTENT

Supporting Information

The Supporting Information is available free of charge at https://pubs.acs.org/doi/10.1021/acs.joc.2c01049.

UV−vis spectra, HPLC traces, GC chromatograms, MIMS analysis, UPLC-MS traces, mass spectra, and ^{31}P NMR spectra (PDF)

■ AUTHOR INFORMATION

Corresponding Author

John P. Toscano − *Department of Chemistry, Johns Hopkins University, Baltimore, Maryland 21218, United States;* orcid.org/0000-0002-4277-3533; Email: jtoscano@jhu.edu

Authors

Sahil C. Aggarwal − *Department of Chemistry, Johns Hopkins University, Baltimore, Maryland 21218, United States*

Vinayak S. Khodade − *Department of Chemistry, Johns Hopkins University, Baltimore, Maryland 21218, United States;* orcid.org/0000-0003-2406-5856

Sarah Porche − *Department of Chemistry, Johns Hopkins University, Baltimore, Maryland 21218, United States*

Blaze M. Pharoah − *Department of Chemistry, Johns Hopkins University, Baltimore, Maryland 21218, United States*

Complete contact information is available at: https://pubs.acs.org/10.1021/acs.joc.2c01049

Notes

The authors declare no competing financial interest.

■ ACKNOWLEDGMENTS

We gratefully acknowledge the National Science Foundation (CHE-1900285) for generous support for this research.

■ REFERENCES

(1) Fukuto, J. M.; Ignarro, L. J.; Nagy, P.; Wink, D. A.; Kevil, C. G.; Feelisch, M.; Cortese-Krott, M. M.; Bianco, C. L.; Kumagai, Y.; Hobbs, A. J.; Lin, J.; Ida, T.; Akaike, T. Biological hydropersulfides and related polysulfides − a new concept and perspective in redox biology. *FEBS Lett.* **2018**, *592*, 2140−2152.

(2) Ida, T.; Sawa, T.; Ihara, H.; Tsuchiya, Y.; Watanabe, Y.; Kumagai, Y.; Suematsu, M.; Motohashi, H.; Fujii, S.; Matsunaga, T.; Yamamoto, M.; Ono, K.; Devarie-Baez Nelmi, O.; Xian, M.; Fukuto Jon, M.; Akaike, T. Reactive cysteine persulfides and S-polythiolation regulate oxidative stress and redox signaling. *Proc. Natl. Acad. Sci. U. S. A.* **2014**, *111*, 7606−7611.

(3) Kunikata, H.; Ida, T.; Sato, K.; Aizawa, N.; Sawa, T.; Tawarayama, H.; Murayama, N.; Fujii, S.; Akaike, T.; Nakazawa, T. Metabolomic profiling of reactive persulfides and polysulfides in the aqueous and vitreous humors. *Sci. Rep.* **2017**, *7*, 41984.

(4) Sawa, T.; Motohashi, H.; Ihara, H.; Akaike, T. Enzymatic Regulation and Biological Functions of Reactive Cysteine Persulfides and Polysulfides. *Biomolecules* **2020**, *10*, 1245.

(5) Yadav, P. K.; Martinov, M.; Vitvitsky, V.; Seravalli, J.; Wedmann, R.; Filipovic, M. R.; Banerjee, R. Biosynthesis and Reactivity of Cysteine Persulfides in Signaling. *J. Am. Chem. Soc.* **2016**, *138*, 289−299.

(6) Akaike, T.; Ida, T.; Wei, F.-Y.; Nishida, M.; Kumagai, Y.; Alam, M. M.; Ihara, H.; Sawa, T.; Matsunaga, T.; Kasamatsu, S.; Nishimura, A.; Morita, M.; Tomizawa, K.; Nishimura, A.; Watanabe, S.; Inaba, K.; Shima, H.; Tanuma, N.; Jung, M.; Fujii, S.; Watanabe, Y.; Ohmuraya, M.; Nagy, P.; Feelisch, M.; Fukuto, J. M.; Motohashi, H. Cysteinyl-tRNA synthetase governs cysteine polysulfidation and mitochondrial bioenergetics. *Nat. Commun.* **2017**, *8*, 1177.

(7) Fukuto, J. M.; Hobbs, A. J. A comparison of the chemical biology of hydropersulfides (RSSH) with other protective biological antioxidants and nucleophiles. *Nitric Oxide* **2021**, *107*, 46−57.

(8) Álvarez, L.; Suarez Vega, V.; McGinity, C.; Khodade, V. S.; Toscano, J. P.; Nagy, P.; Lin, J.; Works, C.; Fukuto, J. M. The reactions of hydropersulfides (RSSH) with myoglobin. *Arch. Biochem. Biophys.* **2020**, *687*, No. 108391.

(9) Benchoam, D.; Semelak, J. A.; Cuevasanta, E.; Mastrogiovanni, M.; Grassano, J. S.; Ferrer-Sueta, G.; Zeida, A.; Trujillo, M.; Möller, M. N.; Estrin, D. A.; Alvarez, B. Acidity and nucleophilic reactivity of glutathione persulfide. *J. Biol. Chem.* **2020**, *295*, 15466−15481.

(10) Zarenkiewicz, J.; Khodade, V. S.; Toscano, J. P. Reaction of Nitroxyl (HNO) with Hydrogen Sulfide and Hydropersulfides. *J. Org. Chem.* **2021**, *86*, 868−877.

(11) Fukuto, J. M.; Lin, J.; Khodade, V. S.; Toscano, J. P. Predicting the Possible Physiological/Biological Utility of the Hydropersulfide Functional Group Based on Its Chemistry: Similarities Between Hydropersulfides and Selenols. *Antioxid. Redox Signaling* **2020**, *33*, 1295−1307.

(12) Takata, T.; Araki, S.; Tsuchiya, Y.; Watanabe, Y. Persulfide Signaling in Stress-Initiated Calmodulin Kinase Response. *Antioxid. Redox Signaling* **2020**, *33*, 1308−1319.

(13) Petrovic, D.; Kouroussis, E.; Vignane, T.; Filipovic, M. R. The Role of Protein Persulfidation in Brain Aging and Neurodegeneration. *Front. Aging Neurosci.* **2021**, *13*, No. 674135.

(14) Khodade, V. S.; Aggarwal, S. C.; Eremiev, A.; Bao, E.; Porche, S.; Toscano, J. P. Development of Hydropersulfide Donors to Study Their Chemical Biology. *Antioxid. Redox Signaling* **2021**, *36*, 309−326.

(15) Dillon, K. M.; Matson, J. B. A Review of Chemical Tools for Studying Small Molecule Persulfides: Detection and Delivery. *ACS Chem. Biol.* **2021**, *16*, 1128−1141.

(16) Kang, J.; Ferrell, A. J.; Chen, W.; Wang, D.; Xian, M. Cyclic Acyl Disulfides and Acyl Selenylsulfides as the Precursors for Persulfides (RSSH), Selenylsulfides (RSeSH), and Hydrogen Sulfide (H2S). *Org. Lett.* **2018**, *20*, 852−855.

(17) Bora, P.; Chauhan, P.; Manna, S.; Chakrapani, H. A Vinyl-Boronate Ester-Based Persulfide Donor Controllable by Hydrogen

Peroxide, a Reactive Oxygen Species (ROS). *Org. Lett.* **2018**, *20*, 7916−7920.
(18) Powell, C. R.; Dillon, K. M.; Wang, Y.; Carrazzone, R. J.; Matson, J. B. A Persulfide Donor Responsive to Reactive Oxygen Species: Insights into Reactivity and Therapeutic Potential. *Angew. Chem., Int. Ed.* **2018**, *57*, 6324−6328.
(19) Hankins, R. A.; Suarez, S. I.; Kalk, M. A.; Green, N. M.; Harty, M. N.; Lukesh Iii, J. C. An Innovative Hydrogen Peroxide-Sensing Scaffold and Insight Towards its Potential as an ROS-Activated Persulfide Donor. *Angew. Chem., Int. Ed.* **2020**, *59*, 22238−22245.
(20) Khodade, V. S.; Toscano, J. P. Development of S-Substituted Thioisothioureas as Efficient Hydropersulfide Precursors. *J. Am. Chem. Soc.* **2018**, *140*, 17333−17337.
(21) Khodade, V. S.; Pharoah, B. M.; Paolocci, N.; Toscano, J. P. Alkylamine-Substituted Perthiocarbamates: Dual Precursors to Hydropersulfide and Carbonyl Sulfide with Cardioprotective Actions. *J. Am. Chem. Soc.* **2020**, *142*, 4309−4316.
(22) Khodade, V. S.; Aggarwal, S. C.; Pharoah, B. M.; Paolocci, N.; Toscano, J. P. Alkylsulfenyl thiocarbonates: precursors to hydropersulfides potently attenuate oxidative stress. *Chem. Sci.* **2021**, *12*, 8252−8259.
(23) Yuan, Z.; Zheng, Y.; Yu, B.; Wang, S.; Yang, X.; Wang, B. Esterase-Sensitive Glutathione Persulfide Donor. *Org. Lett.* **2018**, *20*, 6364−6367.
(24) Dillon, K. M.; Morrison, H. A.; Powell, C. R.; Carrazzone, R. J.; Ringel-Scaia, V. M.; Winckler, E. W.; Council-Troche, R. M.; Allen, I. C.; Matson, J. B. Targeted Delivery of Persulfides to the Gut: Effects on the Microbiome. *Angew. Chem., Int. Ed.* **2021**, *60*, 6061−6067.
(25) Dillon, K. M.; Carrazzone, R. J.; Wang, Y.; Powell, C. R.; Matson, J. B. Polymeric Persulfide Prodrugs: Mitigating Oxidative Stress through Controlled Delivery of Reactive Sulfur Species. *ACS Macro Lett.* **2020**, *9*, 606−612.
(26) Bora, P.; Sathian, M. B.; Chakrapani, H. Enhancing cellular sulfane sulfur through *β*-glycosidase-activated persulfide donors: mechanistic insights and oxidative stress mitigation. *Chem. Commun.* **2022**, *58*, 2987−2990.
(27) Pharoah, B. M.; Khodade, V. S.; Eremiev, A.; Bao, E.; Liu, T.; O'Rourke, B.; Paolocci, N.; Toscano, J. P. Hydropersulfides (RSSH) Outperform Post-Conditioning and Other Reactive Sulfur Species in Limiting Ischemia–Reperfusion Injury in the Isolated Mouse Heart. *Antioxidants* **2022**, *11*, 1010.
(28) Chaudhuri, A.; Venkatesh, Y.; Das, J.; Gangopadhyay, M.; Maiti, T. K.; Singh, N. D. P. One- and Two-Photon-Activated Cysteine Persulfide Donors for Biological Targeting. *J. Org. Chem.* **2019**, *84*, 11441−11449.
(29) Chaudhuri, A.; Venkatesh, Y.; Jena, B. C.; Behara, K. K.; Mandal, M.; Singh, N. D. P. Real-time monitoring of a photoactivated hydrogen persulfide donor for biological entities. *Org. Biomol. Chem.* **2019**, *17*, 8800−8805.
(30) Park, C.-H.; Givens, R. S. New Photoactivated Protecting Groups. 6. p-Hydroxyphenacyl: A Phototrigger for Chemical and Biochemical Probes1,2. *J. Am. Chem. Soc.* **1997**, *119*, 2453−2463.
(31) Zheng, Y.; Yu, B.; Li, Z.; Yuan, Z.; Organ, C. L.; Trivedi, R. K.; Wang, S.; Lefer, D. J.; Wang, B. An Esterase-Sensitive Prodrug Approach for Controllable Delivery of Persulfide Species. *Angew. Chem., Int. Ed.* **2017**, *56*, 11749−11753.
(32) Everett, S. A.; Wardman, P. [5] Perthiols as antioxidants: Radical-scavenging andprooxidative mechanisms. *Methods Enzymol.* **1995**, *251*, 55−69.
(33) Chauvin, J.-P. R.; Griesser, M.; Pratt, D. A. Hydropersulfides: H-Atom Transfer Agents Par Excellence. *J. Am. Chem. Soc.* **2017**, *139*, 6484−6493.
(34) Bianco, C. L.; Chavez, T. A.; Sosa, V.; Saund, S. S.; Nguyen, Q. N. N.; Tantillo, D. J.; Ichimura, A. S.; Toscano, J. P.; Fukuto, J. M. The chemical biology of the persulfide (RSSH)/perthiyl (RSS·) redox couple and possible role in biological redox signaling. *Free Radical Biol. Med.* **2016**, *101*, 20−31.
(35) Klán, P.; Šolomek, T.; Bochet, C. G.; Blanc, A.; Givens, R.; Rubina, M.; Popik, V.; Kostikov, A.; Wirz, J. Photoremovable Protecting Groups in Chemistry and Biology: Reaction Mechanisms and Efficacy. *Chem. Rev.* **2013**, *113*, 119−191.
(36) Toohey, J. I. Persulfide sulfur is a growth factor for cells defective in sulfur metabolism. *Biochem. Cell Biol.* **1986**, *64*, 758−765.
(37) Hoefle, G.; Baldwin, J. E. Thiosulfoxides. Intermediates in rearrangement and reduction of allylic disulfides. *J. Am. Chem. Soc.* **1971**, *93*, 6307−6308.
(38) Kutney, G. W.; Turnbull, K. Compounds containing the sulfur-sulfur double bond. *Chem. Rev.* **1982**, *82*, 333−357.
(39) Toohey, J. I.; Cooper, A. J. L. Thiosulfoxide (Sulfane) Sulfur: New Chemistry and New Regulatory Roles in Biology. *Molecules* **2014**, *19*, 12789−12813.
(40) Liu, C.; Zhang, F.; Munske, G.; Zhang, H.; Xian, M. Isotope dilution mass spectrometry for the quantification of sulfane sulfurs. *Free Radical Biol. Med.* **2014**, *76*, 200−207.
(41) Givens, R. S.; Stensrud, K.; Conrad, P. G.; Yousef, A. L.; Perera, C.; Senadheera, S. N.; Heger, D.; Wirz, J. p-Hydroxyphenacyl photoremovable protecting groups — Robust photochemistry despite substituent diversity. *Can. J. Chem.* **2011**, *89*, 364−384.
(42) Alouane, A.; Labruère, R.; Le Saux, T.; Aujard, I.; Dubruille, S.; Schmidt, F.; Jullien, L. Light Activation for the Versatile and Accurate Kinetic Analysis of Disassembly of Self-Immolative Spacers. *Chem. − Eur. J.* **2013**, *19*, 11717−11724.
(43) Alouane, A.; Labruère, R.; Le Saux, T.; Schmidt, F.; Jullien, L. Self-Immolative Spacers: Kinetic Aspects, Structure−Property Relationships, and Applications. *Angew. Chem., Int. Ed.* **2015**, *54*, 7492−7509.
(44) Weinrich, T.; Gränz, M.; Grünewald, C.; Prisner, T. F.; Göbel, M. W. Synthesis of a Cytidine Phosphoramidite with Protected Nitroxide Spin Label for EPR Experiments with RNA. *Eur. J. Org. Chem.* **2017**, *2017*, 491−496.
(45) Kuhn, H. J.; Braslavsky, S. E.; Schmidt, R. Chemical Actinometry. *Pure Appl. Chem.* **1989**, *61*, 187−210.
(46) Ruane, P. H.; Bushan, K. M.; Pavlos, C. M.; D'S, R. A.; Toscano, J. P. Controlled Photochemical Release of Nitric Oxide from O2-Benzyl-Substituted Diazeniumdiolates. *J. Am. Chem. Soc.* **2002**, *124*, 9806−9811.
(47) Shieh, M.; Ni, X.; Xu, S.; Lindahl, S. P.; Yang, M.; Matsunaga, T.; Flaumenhaft, R.; Akaike, T.; Xian, M. Shining a light on SSP4: A comprehensive analysis and biological applications for the detection of sulfane sulfurs. *Redox Biol.* **2022**, *56*, No. 102433.
(48) Nagata, K. Studies on Thiohydroxamic Acids and Their Metal Chelates. VII. Syntheses of Some Compounds Possessing Mercapto and Hydroxyimino Groups and Their Reactivities with Metal Ions. *Chem. Pharm. Bull.* **1969**, *17*, 661−668.
(49) Salahi, F.; Purohit, V.; Ferraudi, G.; Stauffacher, C.; Wiest, O.; Helquist, P. pHP-Tethered N-Acyl Carbamate: A Photocage for Nicotinamide. *Org. Lett.* **2018**, *20*, 2547−2550.
(50) Bume, D. D.; Pitts, C. R.; Ghorbani, F.; Harry, S. A.; Capilato, J. N.; Siegler, M. A.; Lectka, T. Ketones as directing groups in photocatalytic sp3 C−H fluorination. *Chem. Sci.* **2017**, *8*, 6918−6923.

https://doi.org/10.1021/acs.joc.2c01049
J. Org. Chem. 2022, 87, 12644−12652